Electronic Supplementary Material (ESI) for Materials Horizons.

Supporting information

Photo-Controllable Microcleaner: Photo-Induced Crawling Motion and Particle Transport of Azobenzene Crystals on a Liquid-Like Surface

Makoto Saikawa,[ab] Mio Ohnuma,[b] Kengo Manabe,[b] Koichiro Saito,[b] Yoshihiro Kikkawa [b] and Yasuo Norikane*[bc]

[a] Graduate School of Science and Technology, University of Tsukuba, Tsukuba, Ibaraki 305-8571, Japan
[b] Research Institute for Advanced Electronics and Photonics, National Institute of Advanced Industrial Science and Technology (AIST), Tsukuba, Ibaraki 305-8565, Japan
[c] Faculty of Pure and Applied Sciences, University of Tsukuba, Tsukuba, Ibaraki 305-8571, Japan

*Corresponding Author. E-mail: y-norikane@aist.go.jp

Materials and Methods

DMAB, propyltrimethoxysilane, hexyltrimethoxysilane, decyltrimethoxysilane, hexadecyltrimethoxysilane, and TMOS were purchased from Tokyo Chemical Industry Co., Ltd. 1H,1H,2H,2H-perfluorodecyltriethoxysilane was purchased from Fujifilm Wako Pure Chemical Corporation. Unless otherwise noted, all other solvents and reagents were purchased from Kishida Chemical Co., Ltd. Hydrochloric acid was used after diluting with water. DMAB was purified by performing column chromatography on silica gel using ethyl acetate/n-hexane (1:40) and subsequent recrystallization from methanol. All other reagents were used as received. Silica gel used for column chromatography was purchased from Kanto Chemical Co. Inc. (Silica Gel 60N (spherical, neutral, 40–50 μm)). Silica particles having diameters of 2, 5, 10, and 20 μm were purchased from Ube Exsymo Co., Ltd. (HIPRESICA TS N3N) and used as received.

Cover glasses (Matsunami Glass Ind., Ltd., square microscope cover glass No. 1, 18 mm × 18 mm, thickness: 0.12–0.17 mm) were used as substrates. They were used after cleaning with a UV/ozone cleaner (Nippon Laser & Electronics Lab.). The Hyb3, Hyb6, Hyb10, and Hyb16 films were prepared as per the literature.[S1] The cover glasses were used as substrates, and the curing time was extended to more than 1 week. The TMS10, TMS16, and FAS10 films were prepared by applying spin-coating (3,000 rpm for 45 s) onto a cover glass with a solution of the corresponding silane reagents (1 vol% solution in ethanol) and then curing on a digital hot stirrer (AS ONE Corporation, DP-1S) at 100 °C for 10 min. Spin-coating was performed by using a spin coater (Mikasa Co., Ltd., 1H-D7). Hydrophilic glass was prepared by dipping a cover glass in a saturated KOH/EtOH solution for 1 h, and the glass was then washed with water and EtOH.

Polycrystals of *trans*-DMAB were ground by using a mortar and pestle and scattered on the substrate through a stainless-steel sieve (mesh size: 25 μm) to place similarly sized crystals without disturbing the substrate surface. This method was found to be suitable for the sample preparation in our previous paper.[S2]

To evaluate the motion of the crystals on each substrate, light irradiation was performed with LEDs at 365 nm (CCS Inc., HLV-24UV365-4WNRBTNJ) and 465 nm (CCS Inc., HLV2-22BL-3 W) using the experimental setup described in our previous report.[S2,S3] The lights were placed at an angle of 30° with the plane of the substrate and faced each other. The light intensity was monitored using a Newport 1917-R optical power meter equipped with an 818-ST2-UV photodetector. The intensities of 365 and 465 nm were 200 and 50 mW cm^{-2}, respectively. The motion of the crystals was observed using a KEYENCE VK-X150 laser microscope at a wavelength of 658 nm. Photomicrographs were obtained every minute. The velocity of the crystal motion was measured based on the center of the crystals. The center of the crystal was defined as the centroid of each image. The motion of the crystals under optically

polarized conditions was observed using an Olympus BX51 microscope. The zigzag motion of the crystals was observed using a Nikon Eclipse Ti microscope.

To prepare a random sample for the transport of silica particles, the particles and substrate were placed in a glass vial. The particles were placed on the substrate by blowing air and then by placing the DMAB crystals as described earlier.

The static contact angle (θ_S), sliding angle (θ_α), advancing contact angle (θ_{Adv}), and receding contact angle (θ_{Rec}) for a 10 μL drop of water were measured by using a contact angle meter (Kyowa Interface Science Co., Ltd., DM-500) at room temperature. The water drop was placed using a syringe provided with the instrument. The contact angle hysteresis ($\Delta\theta_{cos}$) was calculated by applying the following equation: $\Delta\theta_{cos} = \cos\theta_{Rec} - \cos\theta_{Adv}$.

The static contact angle (θ_S'), sliding angle (θ_α'), advancing contact angle (θ_{Adv}'), and receding contact angle (θ_{Rec}') for a 3 μL drop of DMAB were measured by using a contact angle meter (Kyowa Interface Science Co., Ltd., DM-500) at room temperature. DMAB crystals were melted on a cool plate at 60 °C (AS ONE Corporation, SCP-85). After being cooled to 25 °C, the drop of DMAB in the supercooled state was gently placed on the substrate using a micropipette. The contact angle hysteresis ($\Delta\theta_{cos}$') was calculated by applying the following equation: $\Delta\theta_{cos}' = \cos\theta_{Rec}' - \cos\theta_{Adv}'$.

AFM images were acquired using an SPI4000/SPA400 system (Seiko Instruments Inc.) to determine the R_{rms} of the surfaces. The OMCL-AC200TS cantilevers (Olympus Corporation) were used for AFM dynamic force mode (tapping) operation. Scanning electron microscopy images were obtained using a JSM-6340F microscope (JEOL Ltd.).

Table S1. The static contact angle (θ_s), sliding angles (θ_α), advancing contact angle (θ_{Adv}), and receding contact angle (θ_{Rec}), and contact angle hysteresis ($\Delta\theta_{cos}$) of the various surfaces. Probe liquid: water (10 µL).

Surface	θ_s / °	θ_α / °	θ_{Adv} / °	θ_{Rec} / °	$\Delta\theta_{cos}$
Hyb3	87	21	92.9	84.5	0.15
Hyb6	101	14	106.1	99.3	0.12
Hyb10	105	13	109.1	103.7	0.09
Hyb16	107	12	110.0	104.9	0.09
TMS10	99	34	104.3	92.4	0.21
TMS16	104	35	110.7	96.3	0.24
FAS10	99 (98[S2])	51	107.2	86.6	0.36
Hydrophilic glass	10 (5[S2])	1	10.6	9.3	0.004

Table S2. The static contact angle (θ_s'), sliding angles (θ_α'), advancing contact angle (θ_{Adv}'), and receding contact angle (θ_{Rec}'), and contact angle hysteresis ($\Delta\theta_{cos}$') of the various surfaces. Probe liquid: melted DMAB (3 µL).

Surface	θ_s' / °	θ_α' / °	θ_{Adv}' / °	θ_{Rec}' / °	$\Delta\theta_{cos}$'
Hyb3	54	26	54.8	47.3	0.102
Hyb6	56	12	56.6	52.9	0.053
Hyb10	53	10	54.3	50.8	0.049
Hyb16	48	15	49.3	45.0	0.055
TMS10	50	15	50.2	45.0	0.067
TMS16	53	20	54.7	49.3	0.074
FAS10	69	33	70.1	61.0	0.144
Hydrophilic glass	13	7	12.7	10.8	0.006

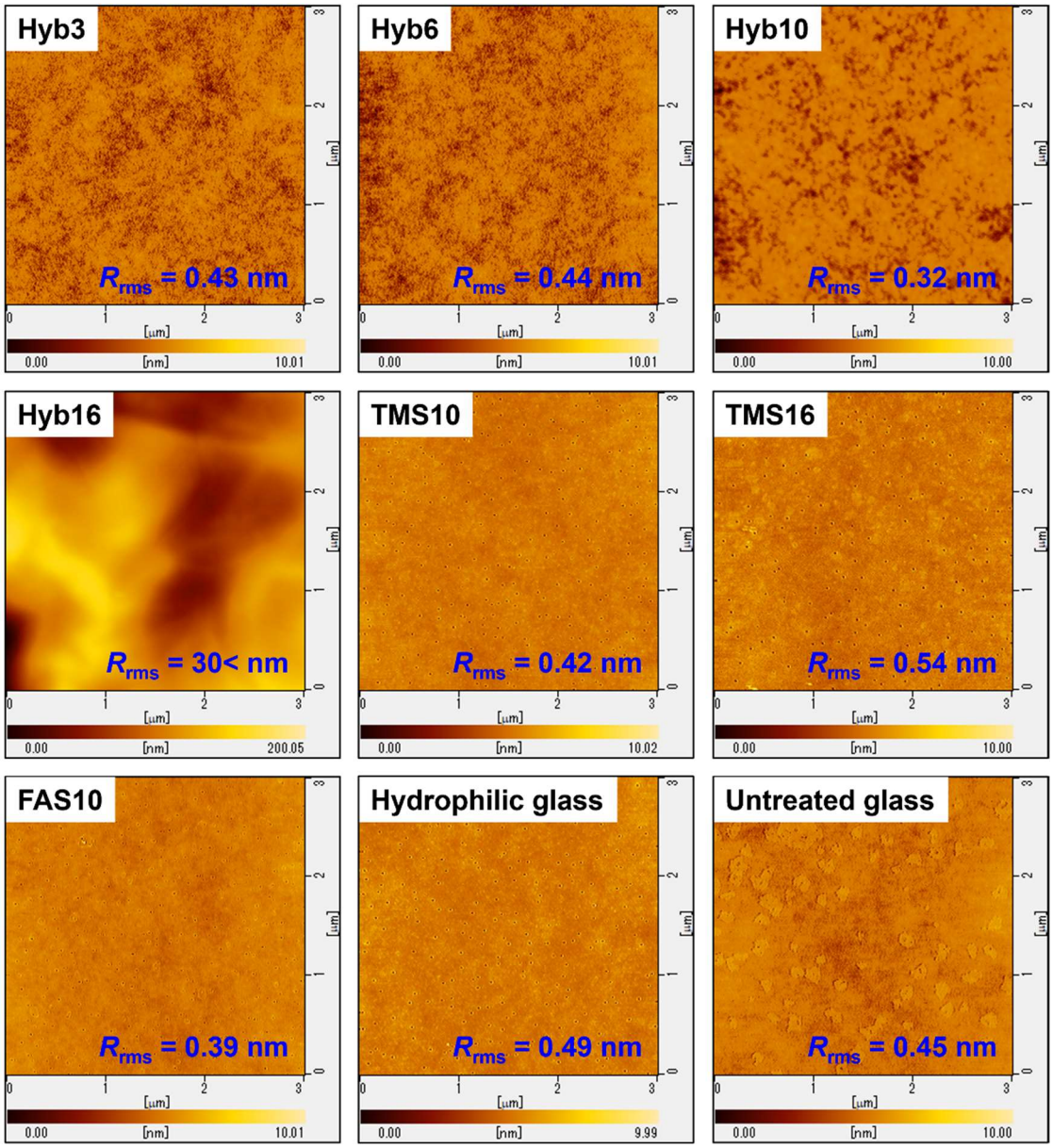

Figure S1. AFM images and the R_{rms} of the various surfaces. Scan area: 3 × 3 μm^2.

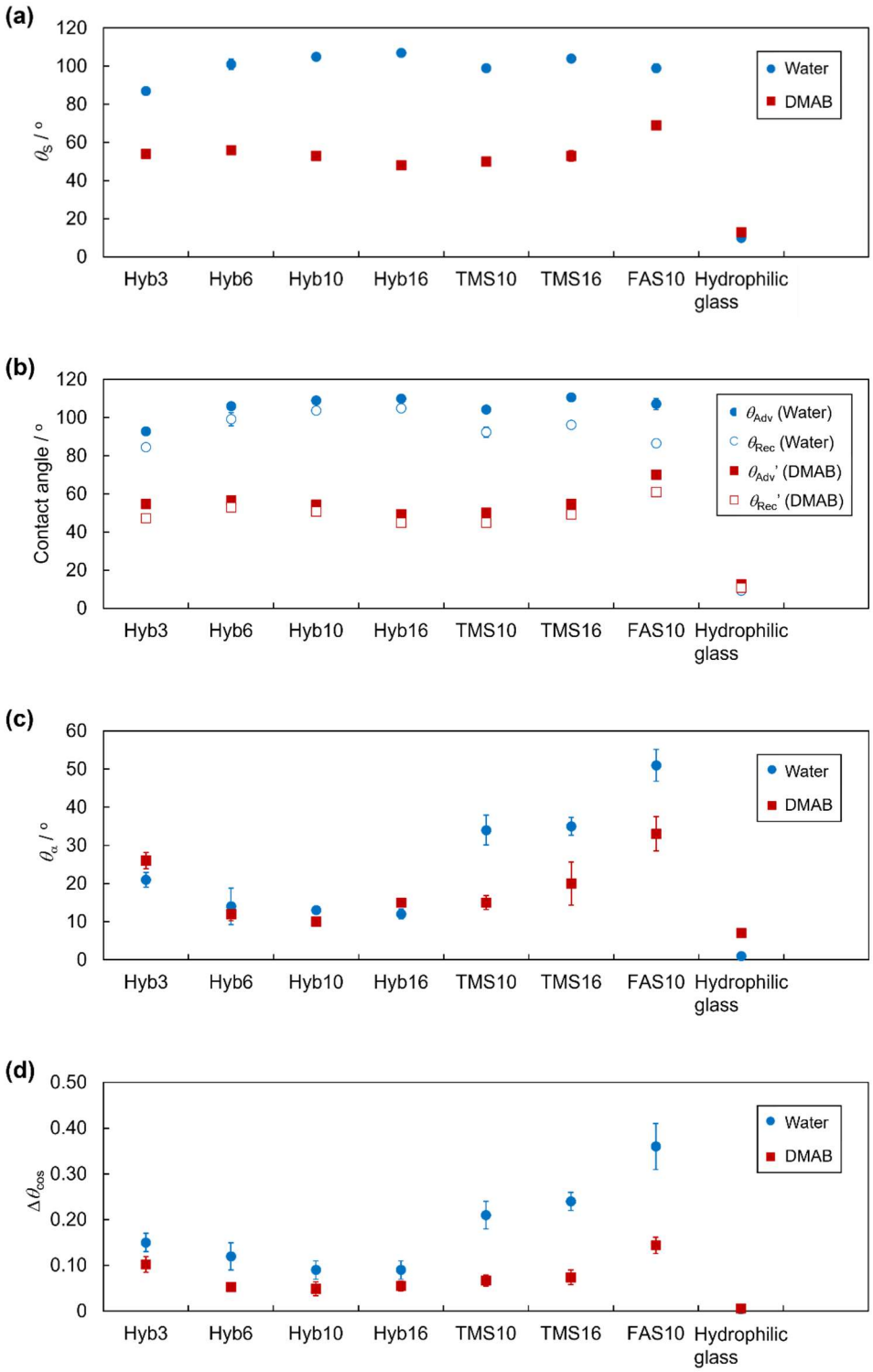

Figure S2. (a) The static contact angle (θ_s), (b) the advancing contact angle (θ_{Adv}) and the receding contact angle (θ_{Rec}), (c) the sliding angle (θ_α), and the contact angle hysteresis ($\Delta\theta_{cos}$) of the various surfaces. Probe liquid: water (10 µL) or melted DMAB (3 µL).

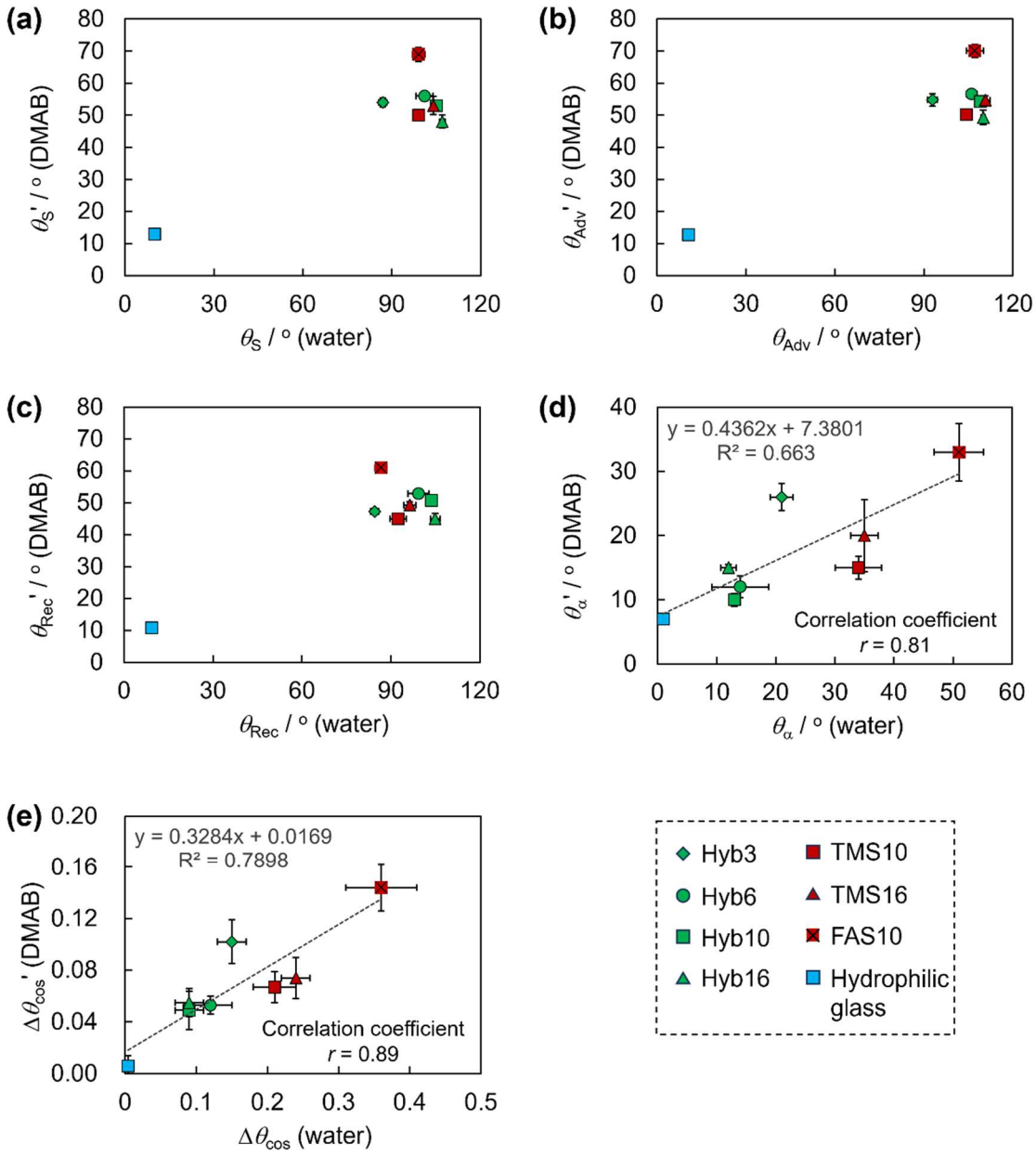

Figure S3. Plots of (a) the static contact angle measured with melted DMAB (θ_s') against that measured with water (θ_s), (b) the advancing contact angle measured with melted DMAB (θ_{Adv}') against that measured with water (θ_{Adv}), (c) the receding contact angle measured with melted DMAB (θ_{Rec}') against that measured with water (θ_{Rec}), (d) the sliding angle measured with melted DMAB (θ_α') against that measured with water (θ_α), and (e) the contact angle hysteresis measured with melted DMAB ($\Delta\theta_{cos}$') against that measured with water ($\Delta\theta_{cos}$).

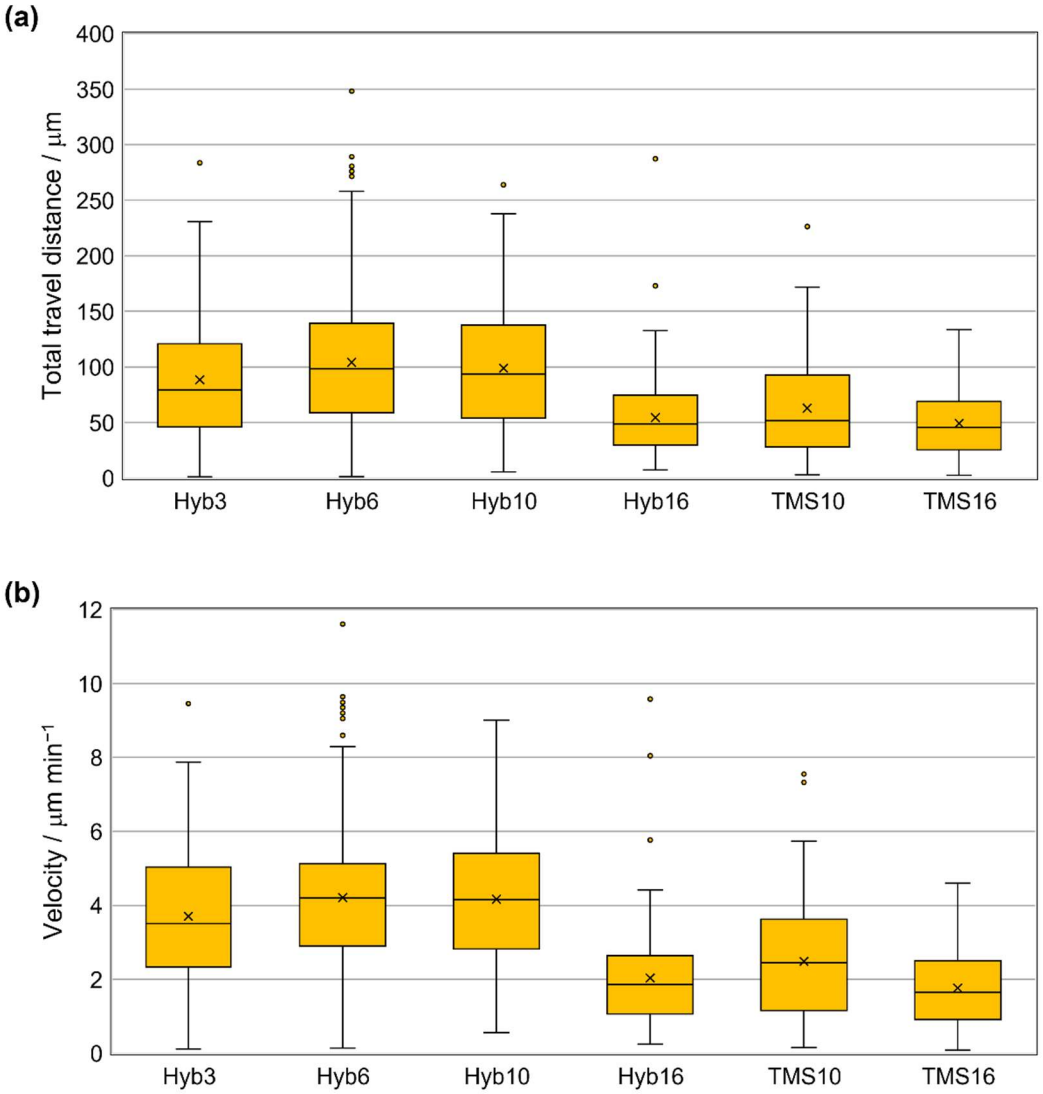

Figure S4. Box plots of (a) the total travel distance and (b) the moving velocity of DMAB crystals on the various surfaces. The boxes show median and first/third quartiles, and the crosses show average.

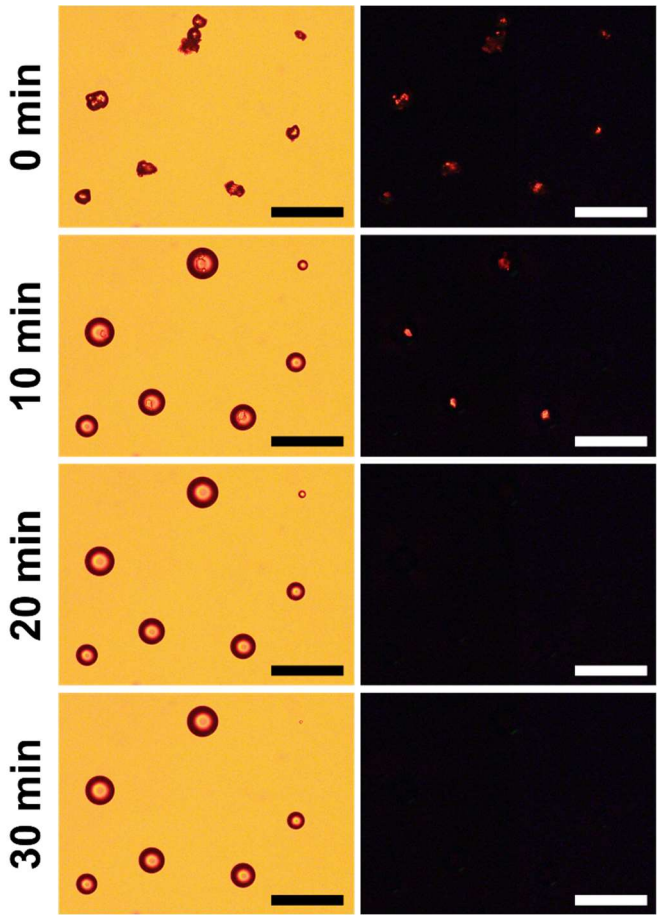

Figure S5. Photomicrographs of DMAB crystals on the Hyb10 film after irradiation for t = 0, 10, 20, and 30 min. The first column presents photomicrographs under bright-field, and the second column shows photomicrographs under polarizing optical microscopes with crossed-polarizer orientation. Light irradiation was performed from the left for UV (365 nm) light. The intensity of 365 nm was 200 mW cm^{-2}. Scale bar: 100 μm.

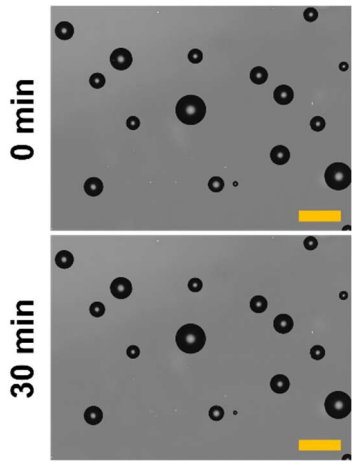

Figure S6. Photomicrographs of DMAB droplets on the Hyb10 film after irradiation for t = 0 and 30 min. Light irradiation was performed from the left for UV (365 nm) light and from the right for visible (465 nm) light. The intensities of 365 and 465 nm were 200 and 50 mW cm^{-2}, respectively. Scale bar: 100 μm.

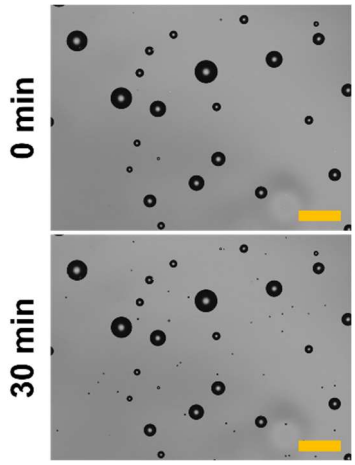

Figure S7. Photomicrographs for DMAB droplets on the Hyb10 film after irradiation for t = 0 and 30 min. Light irradiation was performed from the right for visible (465 nm) light. The intensity of 465 nm was 50 mW cm^{-2}. Scale bar: 100 μm.

When droplets of *trans*-DMAB in a supercooled state were exposed to UV and visible light at 25 °C, the droplets did not exhibit crawling motion (Figure S6). When the droplets were exposed to visible light at 25 °C, they did not exhibit crawling motion, which is in contrast to Figure 2 (Figure S7).

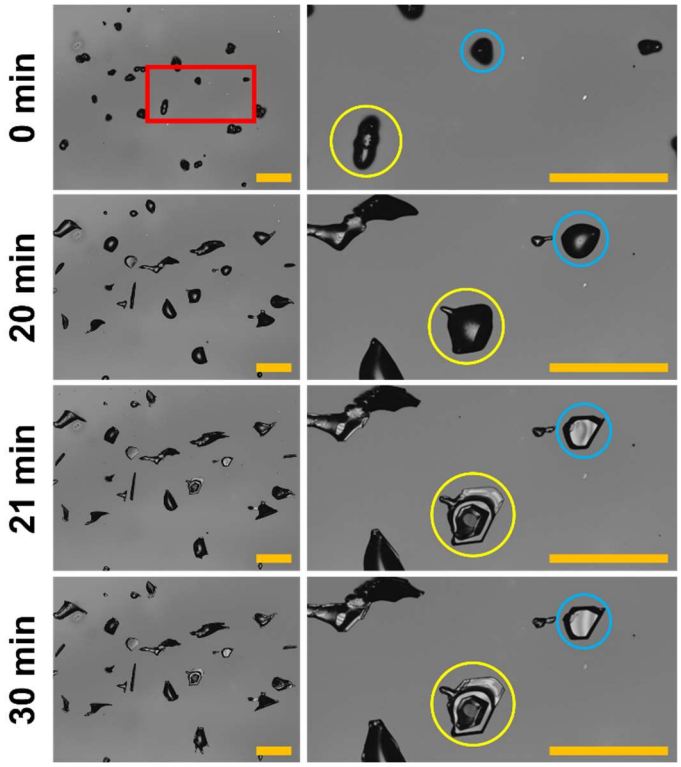

Figure S8. Photomicrographs of DMAB crystals on the Hyb10 film after irradiation for t = 0, 20, 21, and 30 min. The first column presents photomicrographs of the entire field of view, and the second column shows enlarged images of the square in the first column. Light irradiation was performed from the left for UV (365 nm) light and from the right for visible (465 nm) light. The intensities of 365 and 465 nm were 200 and 50 mW cm^{-2} (0−20 min), and 0 and 50 mW cm^{-2} (after 20 min), respectively. Scale bar: 100 μm.

After 20 min of exposure to UV and visible light to continue the crawling motion, the UV light was turned off and only the visible light was irradiated to the crawling DMAB. As soon as only visible light was irradiated, the crawling DMAB stopped crawling and the droplet-like shape changed to an angular shape, indicating the crawling DMAB had recrystallized.

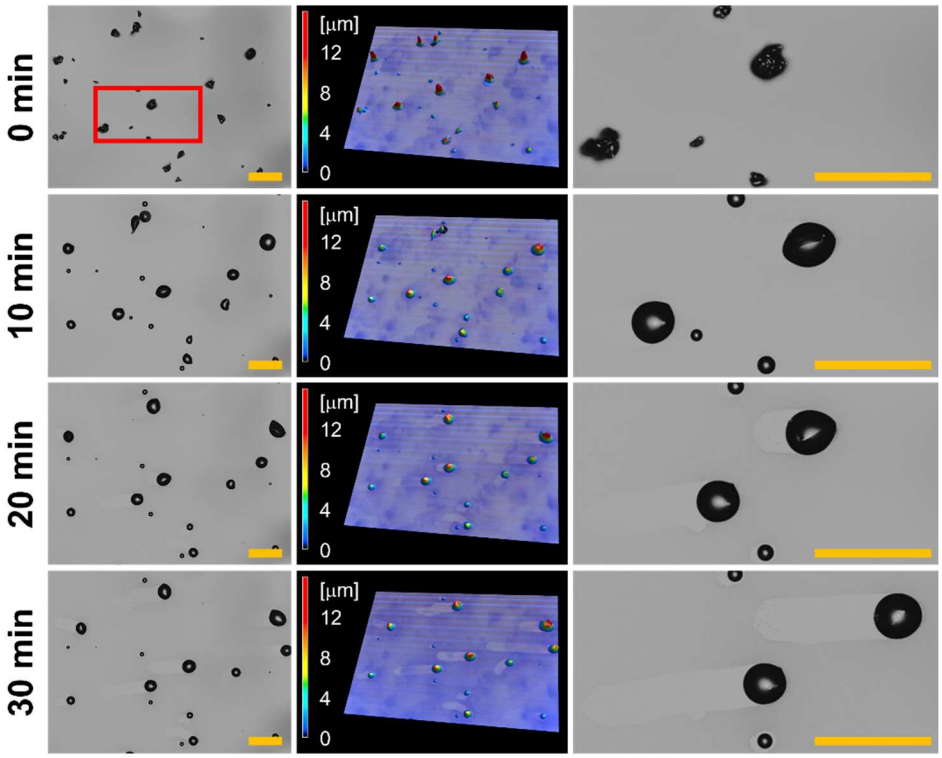

Figure S9. Photomicrographs of the crawling motion of DMAB crystals on the Hyb3 film after irradiation for *t* = 0, 10, 20, and 30 min. The first column presents the photomicrographs of the entire field of view, second column shows 3D images obtained by using a laser scanning microscope, and third column depicts enlarged images of the square in the first column. Light irradiation was performed from the left for UV (365 nm) light and from the right for visible (465 nm) light. The intensities of 365 and 465 nm were 200 and 50 mW cm^{-2}, respectively. Scale bar: 100 μm.

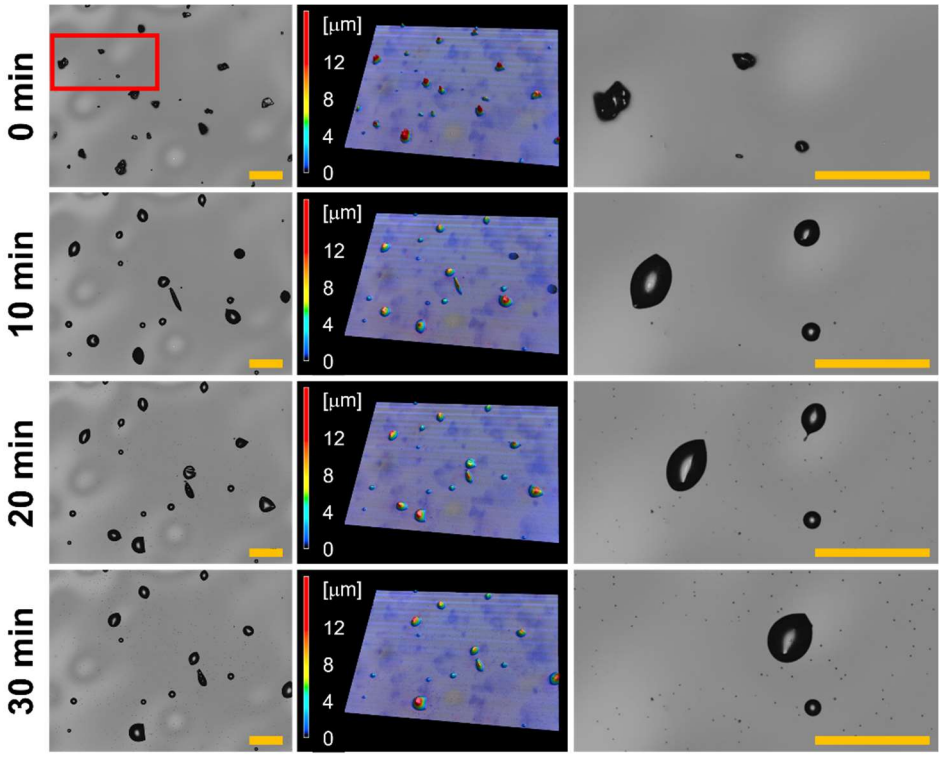

Figure S10. Photomicrographs of the crawling motion of DMAB crystals on the Hyb6 film after irradiation for t = 0, 10, 20, and 30 min. The first column presents the photomicrographs of the entire field of view, second column shows 3D images obtained by using a laser scanning microscope, and third column depicts enlarged images of the square in the first column. Light irradiation was performed from the left for UV (365 nm) light and from the right for visible (465 nm) light. The intensities of 365 and 465 nm were 200 and 50 mW cm^{-2}, respectively. Scale bar: 100 μm.

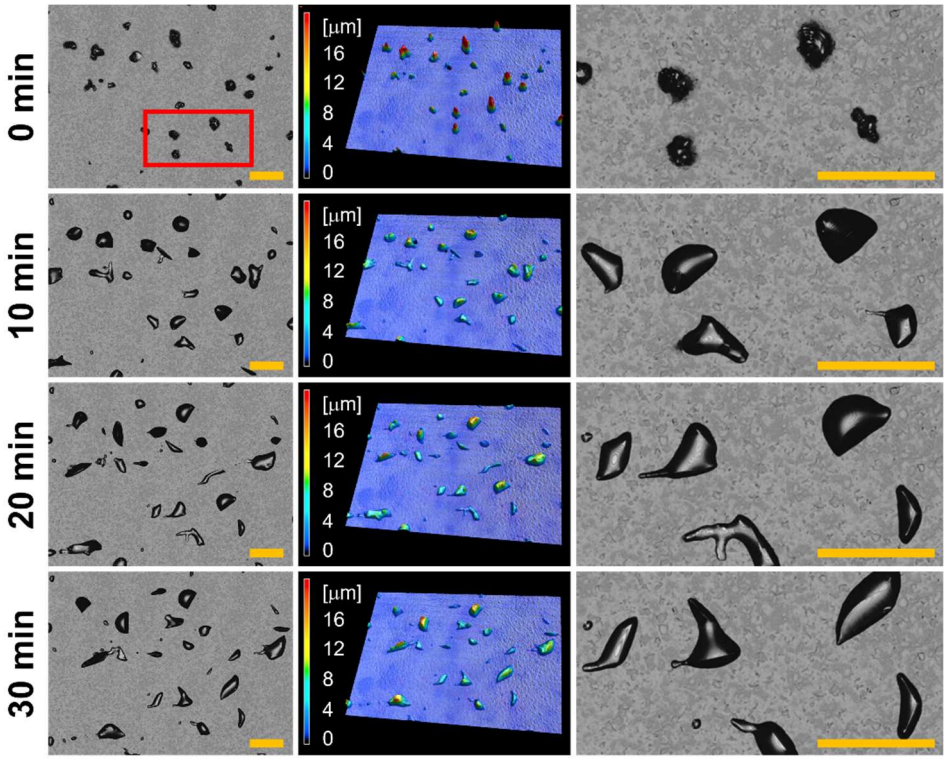

Figure S11. Photomicrographs of the crawling motion of DMAB crystals on the Hyb16 film after irradiation for t = 0, 10, 20, and 30 min. The first column presents the photomicrographs of the entire field of view, second column shows 3D images obtained by using a laser scanning microscope, and third column depicts enlarged images of the square in the first column. Light irradiation was performed from the left for UV (365 nm) light and from the right for visible (465 nm) light. The intensities of 365 and 465 nm were 200 and 50 mW cm^{-2}, respectively. Scale bar: 100 μm.

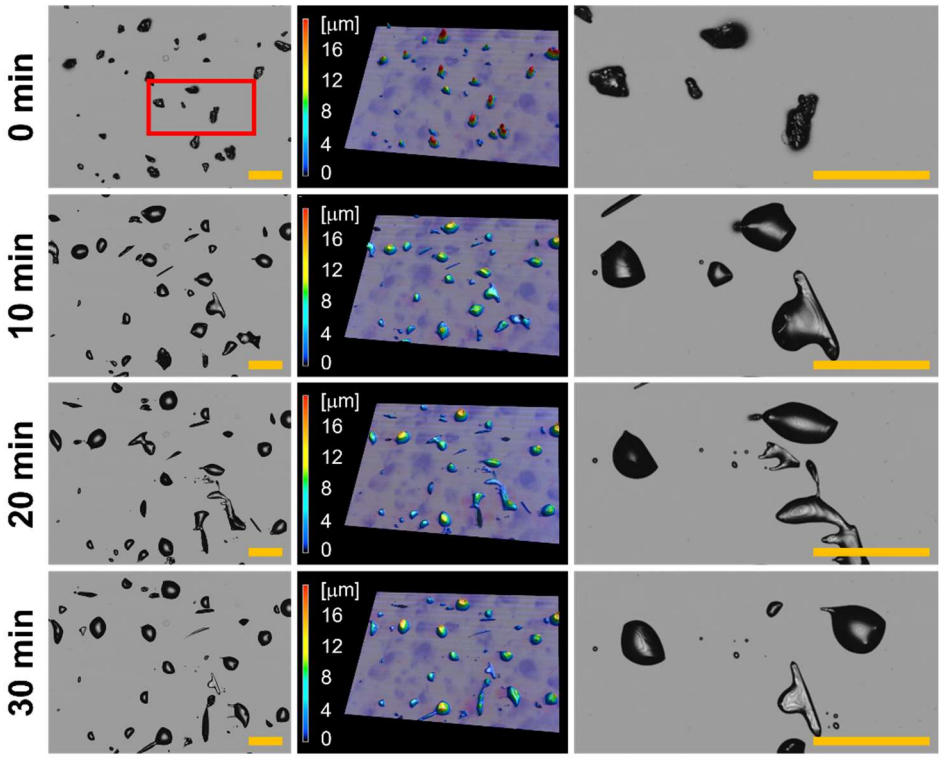

Figure S12. Photomicrographs of the crawling motion of DMAB crystals on the TMS10 film after irradiation for t = 0, 10, 20, and 30 min. The first column presents the photomicrographs of the entire field of view, second column shows 3D images obtained by using a laser scanning microscope, and third column depicts enlarged images of the square in the first column. Light irradiation was performed from the left for UV (365 nm) light and from the right for visible (465 nm) light. The intensities of 365 and 465 nm were 200 and 50 mW cm^{-2}, respectively. Scale bar: 100 μm.

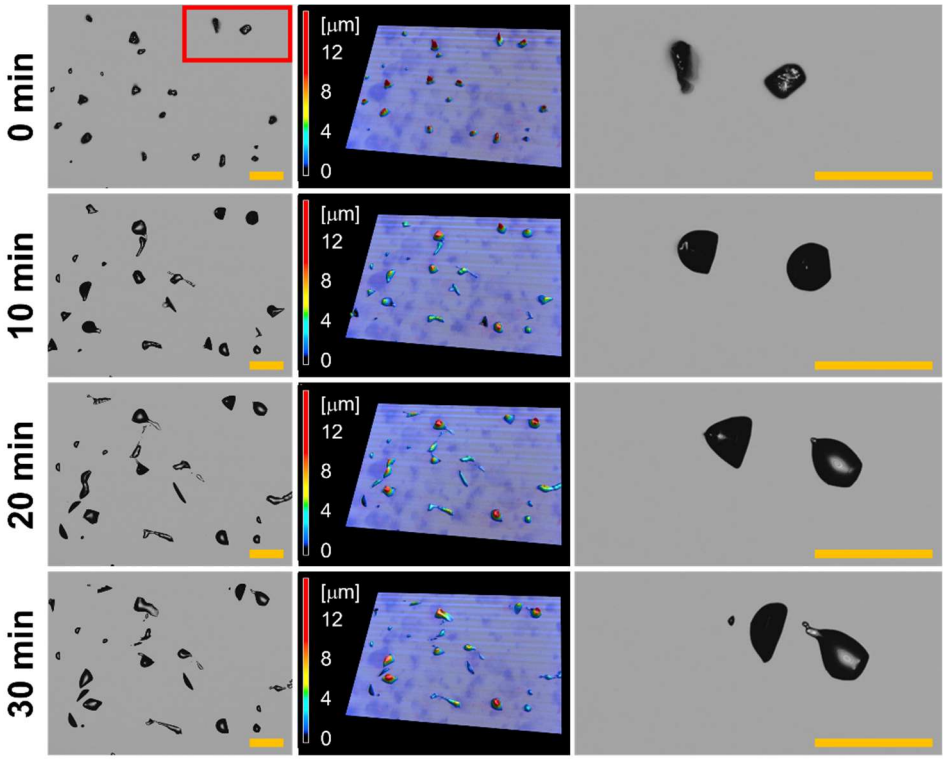

Figure S13. Photomicrographs of the crawling motion of DMAB crystals on the TMS16 film after irradiation for t = 0, 10, 20, and 30 min. The first column presents the photomicrographs of the entire field of view, second column shows 3D images obtained by using a laser scanning microscope, and third column depicts enlarged images of the square in the first column. Light irradiation was performed from the left for UV (365 nm) light and from the right for visible (465 nm) light. The intensities of 365 and 465 nm were 200 and 50 mW cm^{-2}, respectively. Scale bar: 100 μm.

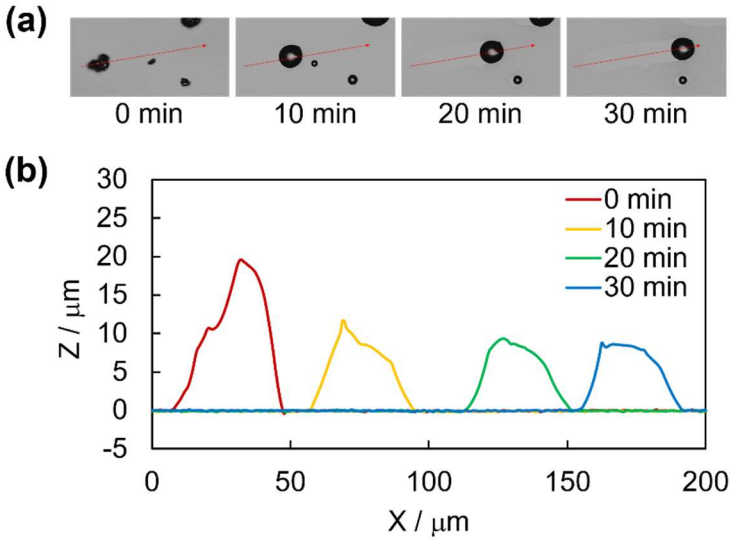

Figure S14. Height profiles of crawling DMAB crystals on the Hyb3 film observed by using laser confocal microscope. (a) Photomicrographs of DMAB crystals on the Hyb3 film after irradiation for *t* = 0, 10, 20, and 30 min. (b) Height profiles of the DMAB crystals along the red arrow in (a) after irradiation for *t* = 0, 10, 20, and 30 min.

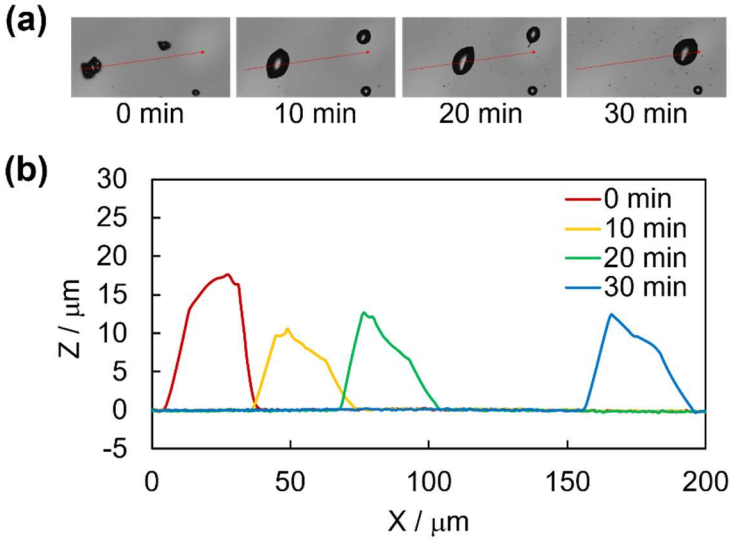

Figure S15. Height profiles of crawling DMAB crystals on the Hyb6 film observed by using laser confocal microscope. (a) Photomicrographs of DMAB crystals on the Hyb6 film after irradiation for *t* = 0, 10, 20, and 30 min. (b) Height profiles of the DMAB crystals along the red arrow in (a) after irradiation for *t* = 0, 10, 20, and 30 min.

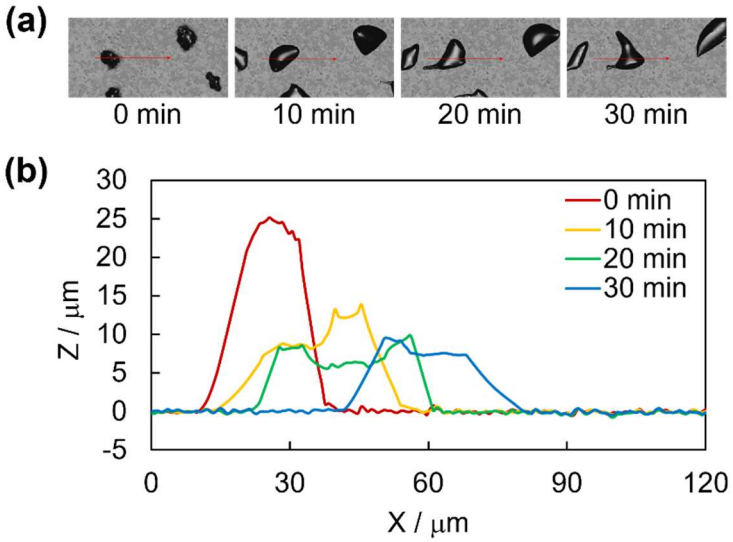

Figure S16. Height profiles of crawling DMAB crystals on the Hyb16 film observed by using laser confocal microscope. (a) Photomicrographs of DMAB crystals on the Hyb16 film after irradiation for *t* = 0, 10, 20, and 30 min. (b) Height profiles of the DMAB crystals along the red arrow in (a) after irradiation for *t* = 0, 10, 20, and 30 min.

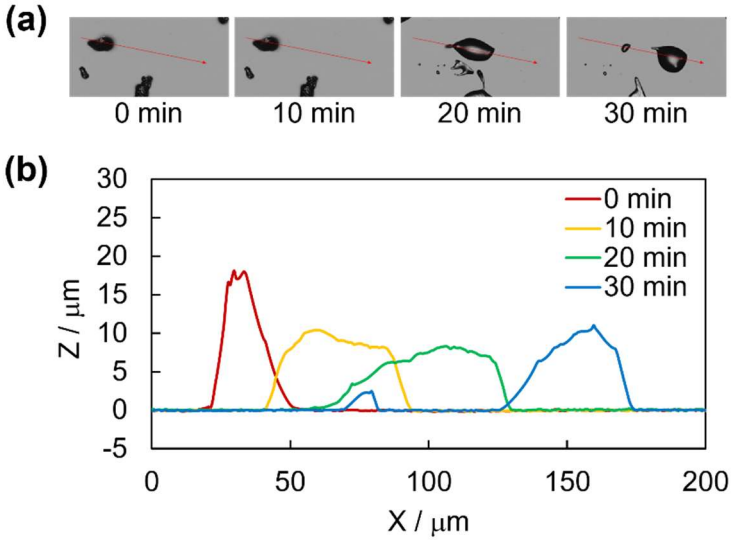

Figure S17. Height profiles of crawling DMAB crystals on the TMS10 film observed by using laser confocal microscope. (a) Photomicrographs of DMAB crystals on the TMS10 film after irradiation for *t* = 0, 10, 20, and 30 min. (b) Height profiles of the DMAB crystals along the red arrow in (a) after irradiation for *t* = 0, 10, 20, and 30 min.

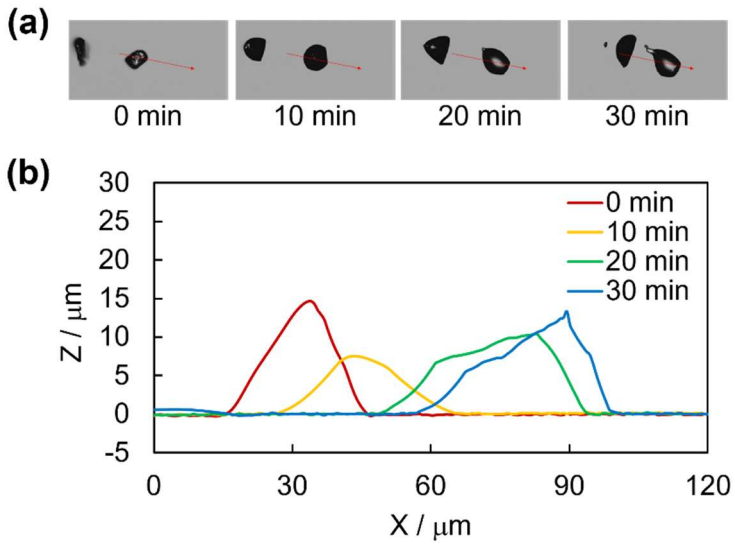

Figure S18. Height profiles of crawling DMAB crystals on the TMS16 film observed by using laser confocal microscope. (a) Photomicrographs of DMAB crystals on the TMS16 film after irradiation for *t* = 0, 10, 20, and 30 min. (b) Height profiles of the DMAB crystals along the red arrow in (a) after irradiation for *t* = 0, 10, 20, and 30 min.

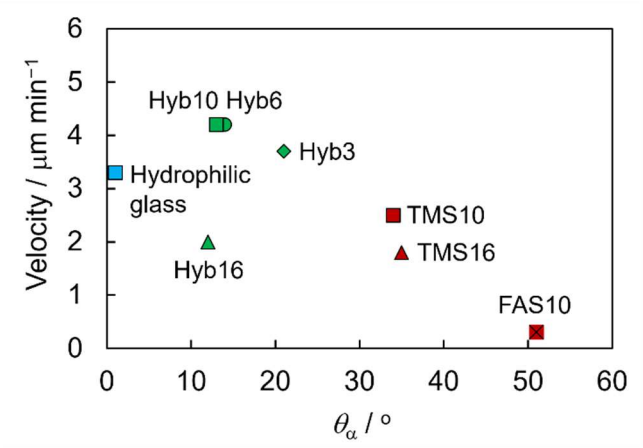

Figure S19. Plots of the moving velocity of DMAB crystals against the sliding angle (θ_α). Probe liquid: water (10 μL).

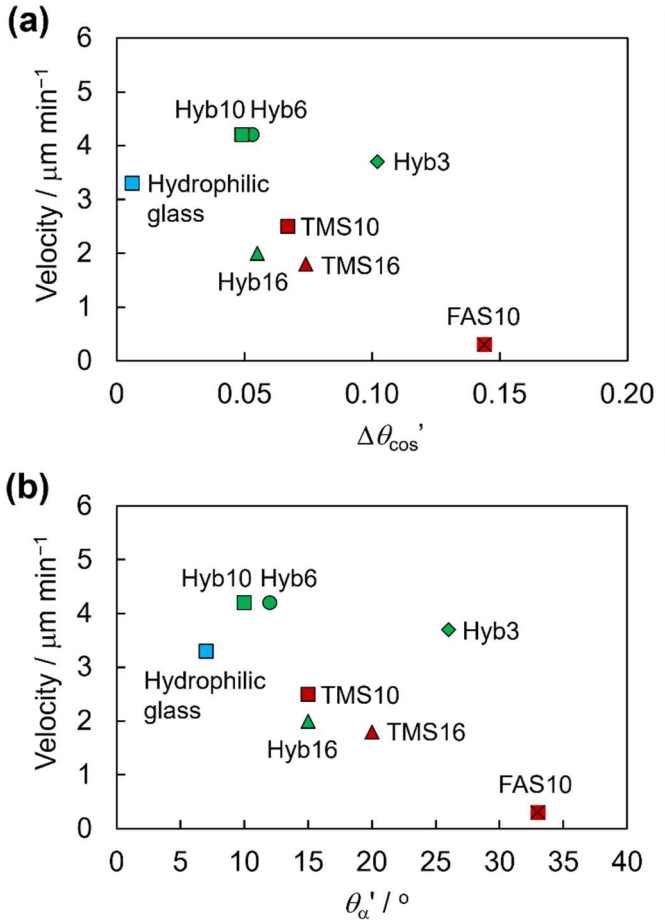

Figure S20. Plots of the moving velocity of DMAB crystals against (a) the contact angle hysteresis ($\Delta\theta_{cos}$') and (b) the sliding angle (θ_α'). Probe liquid: melted DMAB (3 μL).

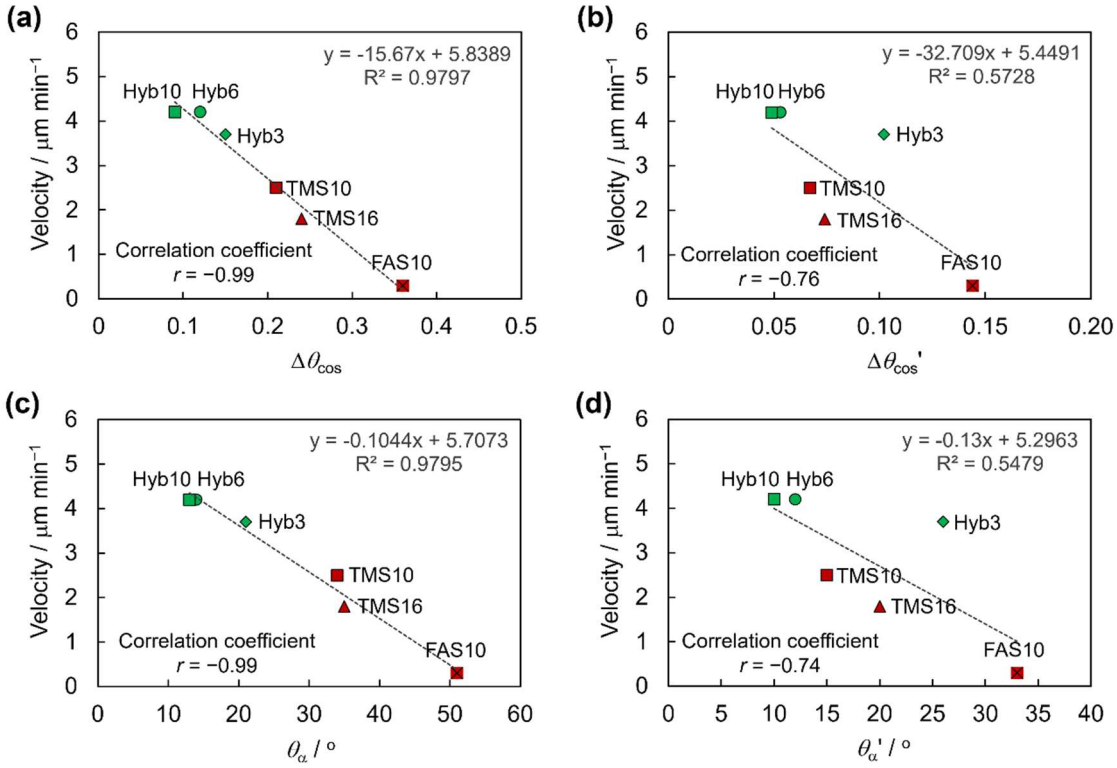

Figure S21. Correlation of the moving velocity of DMAB crystals against the contact angle hysteresis measured with (a) water ($\Delta\theta_{cos}$) in Figure 5 and (b) melted DMAB ($\Delta\theta_{cos}$') in Figure S19, and sliding angle measured with (c) water (θ_α) in Figure S20a and melted DMAB (θ_α') in Figure S20b. The plots corresponding to Hyb16 and hydrophilic glass were omitted to draw the approximate straight line.

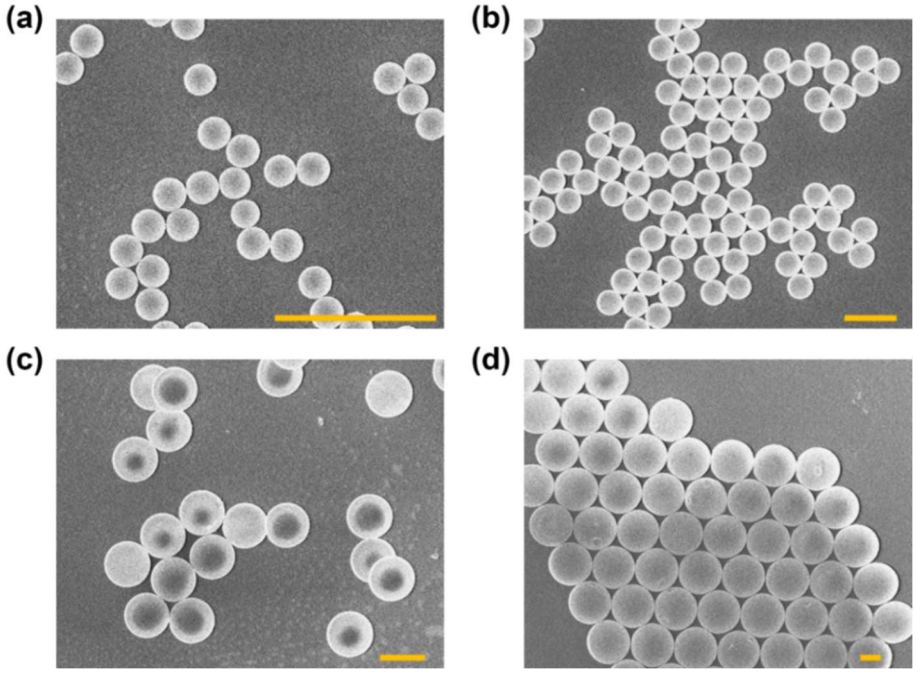

Figure S22. SEM images of silica particles having a diameter of (a) 2 μm, (b) 5 μm, (c) 10 μm, and (d) 20 μm. Scale bar: 10 μm.

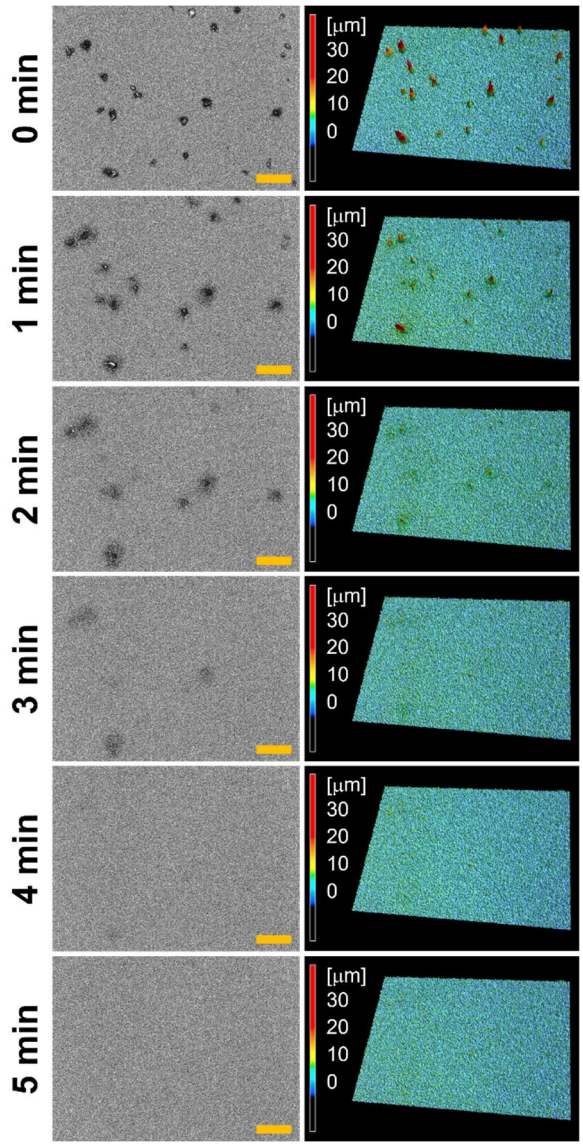

Figure S23. Photomicrographs of DMAB crystals on a heap of silica particles having a diameter of 2 μm after UV (365 nm) light irradiation for t = 0, 1, 2, 3, 4 and 5 min. The first column presents photomicrographs of the entire field of view, and the second column shows 3D images obtained by using a laser scanning microscope. The intensity of 365 nm was 200 mW cm^{-2}. Scale bar: 100 μm.

DMAB crystals were placed on a heap of the silica particles with a diameter of 2 μm and were irradiated with UV light at 200 mW cm^{-2}. Upon the light irradiation, the crystals melted and were adsorbed into the spaces between the particles, resulting in complete disappearance of the DMAB crystals after irradiation for 5 min.

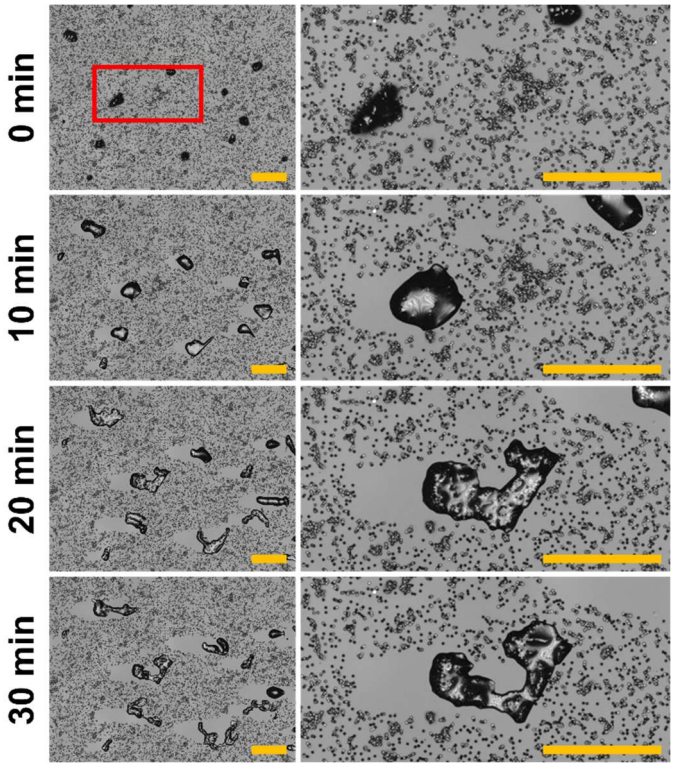

Figure S24. Photomicrographs of the crawling motion of DMAB crystals on the Hyb10 film where large amounts of silica particles having a diameter of 2 μm were placed after irradiation for t = 0, 10, 20, and 30 min. The first column presents photomicrographs of the entire field of view, and the second column shows enlarged images of the square in the first column. Light irradiation was performed from the left for UV (365 nm) light and from the right for visible (465 nm) light. The intensities of 365 and 465 nm were 200 and 50 mW cm^{-2}, respectively. Scale bar: 100 μm.

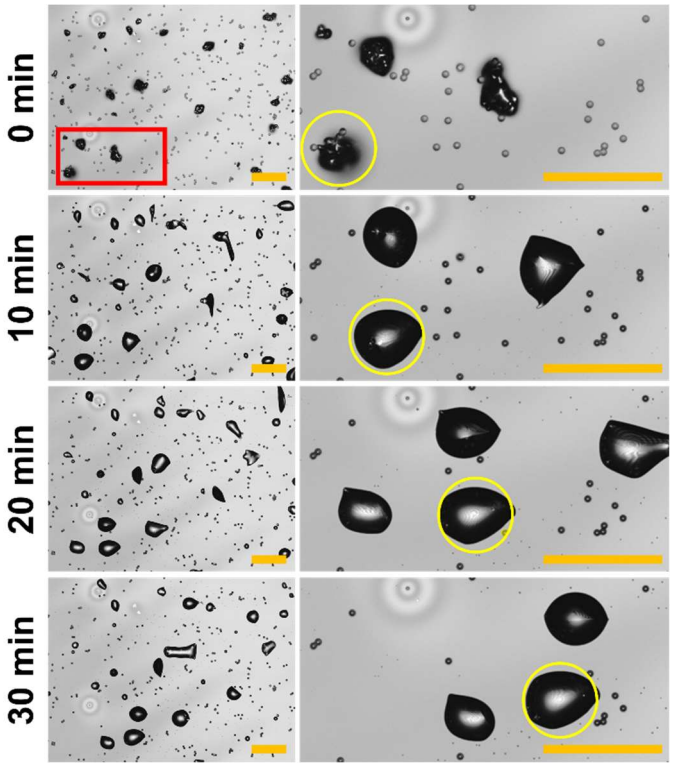

Figure S25. Photomicrographs of the crawling motion of DMAB crystals on the Hyb10 film where silica particles having a diameter of 5 μm were placed after irradiation for t = 0, 10, 20, and 30 min. The first column presents photomicrographs of the entire field of view, and the second column shows enlarged images of the square in the first column. Light irradiation was performed from the left for UV (365 nm) light and from the right for visible (465 nm) light. The intensities of 365 and 465 nm were 200 and 50 mW cm^{-2}, respectively. Scale bar: 100 μm.

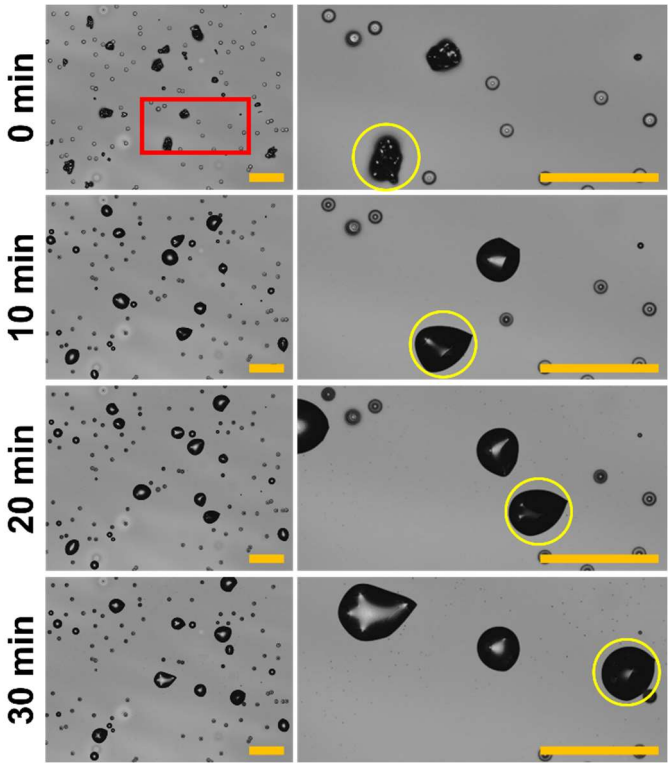

Figure S26. Photomicrographs of the crawling motion of DMAB crystals on the Hyb10 film where silica particles having a diameter of 10 μm were placed after irradiation for t = 0, 10, 20, and 30 min. The first column presents photomicrographs of the entire field of view, and the second column shows enlarged images of the square in the first column. Light irradiation was performed from the left for UV (365 nm) light and from the right for visible (465 nm) light. The intensities of 365 and 465 nm were 200 and 50 mW cm^{-2}, respectively. Scale bar: 100 μm.

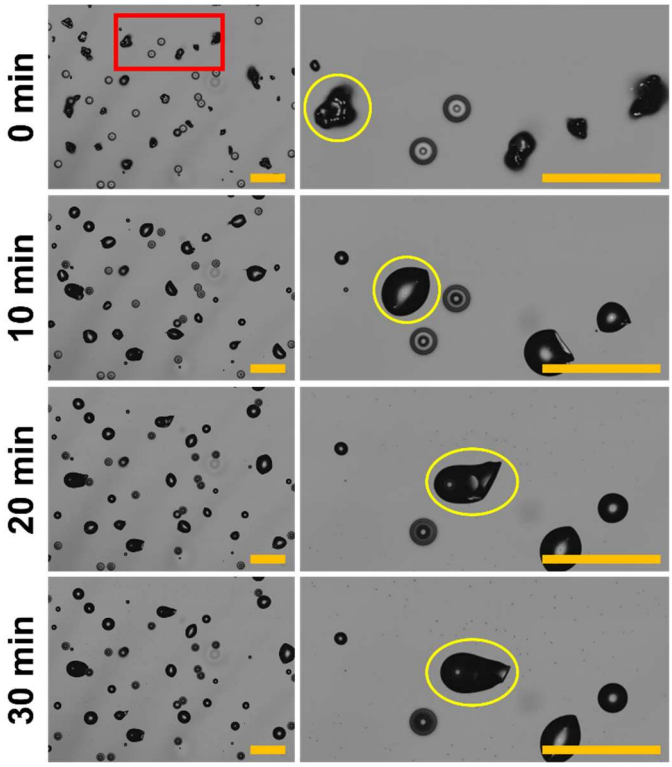

Figure S27. Photomicrographs of the crawling motion of DMAB crystals on the Hyb10 film where silica particles having a diameter of 20 μm were placed after irradiation for t = 0, 10, 20, and 30 min. The first column presents photomicrographs of the entire field of view, and the second column shows enlarged images of the square in the first column. Light irradiation was performed from the left for UV (365 nm) light and from the right for visible (465 nm) light. The intensities of 365 and 465 nm were 200 and 50 mW cm^{-2}, respectively. Scale bar: 100 μm.

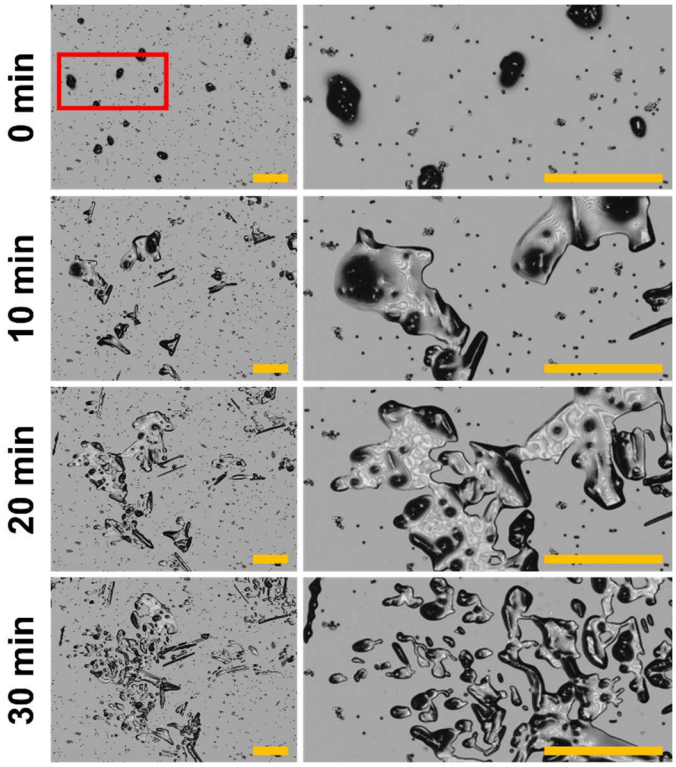

Figure S28. Photomicrographs of the crawling motion of DMAB crystals on the hydrophilic glass where silica particles having a diameter of 2 μm were placed after irradiation for t = 0, 10, 20, and 30 min. The first column presents photomicrographs of the entire field of view, and the second column shows enlarged images of the square in the first column. Light irradiation was performed from the left for UV (365 nm) light and from the right for visible (465 nm) light. The intensities of 365 and 465 nm were 200 and 50 mW cm^{-2}, respectively. Scale bar: 100 μm.

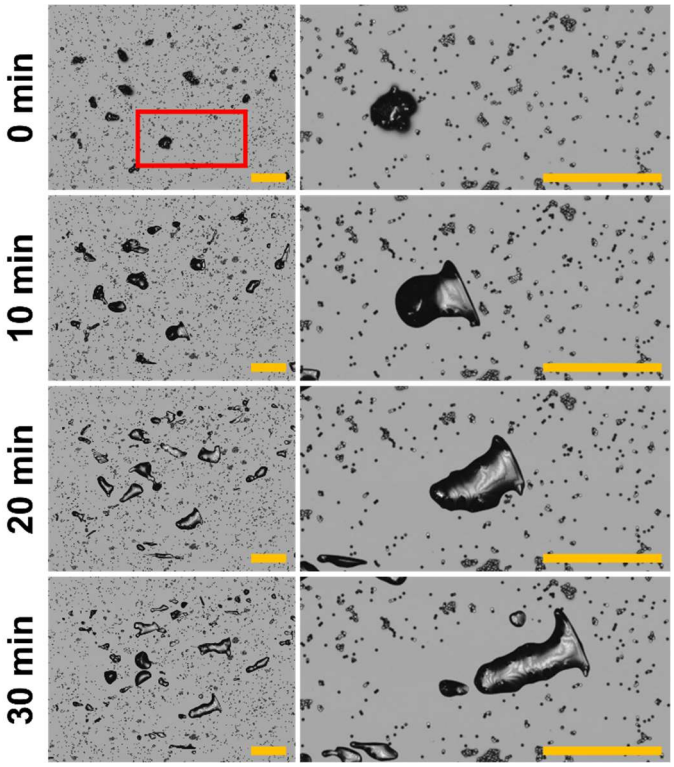

Figure S29. Photomicrographs of the crawling motion of DMAB crystals on the TMS10 film where silica particles having a diameter of 2 μm were placed after irradiation for t = 0, 10, 20, and 30 min. The first column presents photomicrographs of the entire field of view, and the second column shows enlarged images of the square in the first column. Light irradiation was performed from the left for UV (365 nm) light and from the right for visible (465 nm) light. The intensities of 365 and 465 nm were 200 and 50 mW cm^{-2}, respectively. Scale bar: 100 μm.

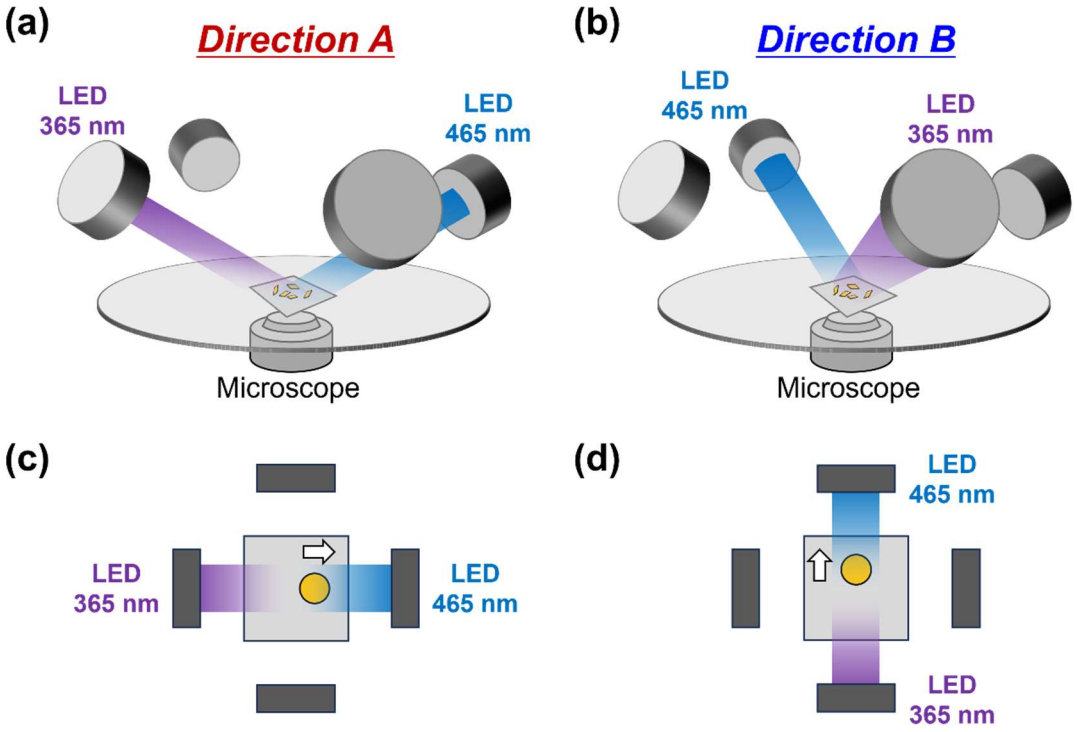

Figure S30. Schematic illustrations of experimental setup for observing the “zigzag” crawling motion of DMAB crystals. (a) The 1st irradiation (0–20 min) and 3rd irradiation (40–60 min) was performed from the left for UV (365 nm) light and from the right for visible (465 nm) light. (b) The 2nd light irradiation (20–40 min) was performed from the front for UV (365 nm) light and from the back for visible (465 nm) light. (c) and (d) Top view of the set up shown in (a) and (b), respectively. The arrows indicate the direction in which the DMAB crystals were moving.

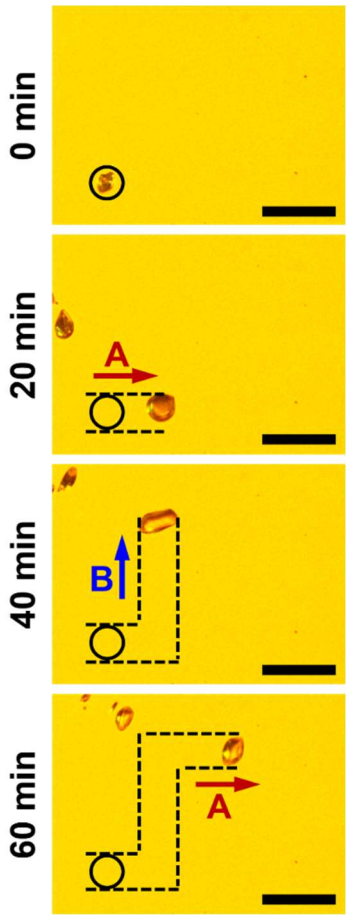

Figure S31. Photomicrographs of the "zigzag" crawling motion of DMAB crystals on the Hyb10 film after irradiation for t = 0, 20, 40, and 60 min. The 1st irradiation (0–20 min) and 3rd irradiation (40–60 min) was performed from the left for UV (365 nm) light and from the right for visible (465 nm) light. The 2nd light irradiation (20–40 min) was performed from the bottom for UV (365 nm) light and from the top for visible (465 nm) light. The intensities of 365 and 465 nm were 200 and 50 mW cm^{-2}, respectively. The arrows and letters (A or B) in the photomicrographs indicate the direction in which the DMAB crystals were moving. Scale bar: 100 μm.

Reference

[S1] C. Urata, B. Masheder, D. F. Cheng and A. Hozumi, *Langmuir*, 2012, **28**, 17681–17689.

[S2] Y. Norikane, M. Hayashino, M. Ohnuma, K. Abe, Y. Kikkawa, K. Saito, K. Manabe, K. Miyake, M. Nakano and N. Takada, *Front Chem*, 2021, **9**, 684767.

[S3] Y. Norikane, M. Hayashino, M. Ohnuma, K. Abe, Y. Kikkawa, K. Saito, K. Manabe, K. Miyake, M. Nakano and N. Takada, *Langmuir*, 2021, **37**, 14177–14185.

Supplementary movies

Movie S1. Crawling motion of DMAB crystals on the Hyb10 film.

Movie S2. Crawling motion of DMAB crystals on the Hyb3 film.

Movie S3. Crawling motion of DMAB crystals on the Hyb6 film.

Movie S4. Crawling motion of DMAB crystals on the Hyb16 film.

Movie S5. Crawling motion of DMAB crystals on the TMS10 film.

Movie S6. Crawling motion of DMAB crystals on the TMS16 film.

Movie S7. Crawling motion of DMAB crystals on the Hyb10 film with 2 μm silica particles.

Movie S8. Crawling motion of DMAB crystals on the Hyb10 film with large amounts of 2 μm silica particles.

Movie S9. Crawling motion of DMAB crystals on the Hyb10 film with 5 μm silica particles.

Movie S10. Crawling motion of DMAB crystals on the Hyb10 film with 10 μm silica particles.

Movie S11. Crawling motion of DMAB crystals on the Hyb10 film with 20 μm silica particles.

Movie S12. Crawling motion of DMAB crystals on the hydrophilic glass with 2 μm silica particles.

Movie S13. Crawling motion of DMAB crystals on the TMS10 film with 2 μm silica particles.

Movie S14. “Zigzag” crawling motion of DMAB crystals on the Hyb10 film.

Movie S15. “Zigzag” crawling motion of DMAB crystals on the Hyb10 film with 2 μm silica particles.